JVI Journals.ASM.org

# The Oncogenic MicroRNA OncomiR-21 Overexpressed during Marek's Disease Lymphomagenesis Is Transactivated by the Viral Oncoprotein Meq

**Grégoire Stik,[a] Ginette Dambrine,[a,b] Sébastien Pfeffer,[c] Denis Rasschaert[a]**

Transcription Lymphome Viro-Induit, UMR 7261 CNRS/University François Rabelais, Tours, France[a]; INRA, Département de Santé Animale, Centre de Recherches de Tours, Nouzilly, France[b]; Architecture et Réactivité de l'ARN, University of Strasbourg, Institut de Biologie Moléculaire et Cellulaire du CNRS Strasbourg, Strasbourg, France[c]

**Gallid herpesvirus 2 (GaHV-2) is an oncogenic herpesvirus that causes T lymphoma in chicken. GaHV-2 encodes a basic leucine zipper (bZIP) protein of the AP-1 family, Meq. Upon formation of homo- or heterodimers with c-Jun, Meq may modulate the expression of viral and cellular genes involved in lymphomagenesis. GaHV-2 also encodes viral microRNAs (miRNAs) involved in latency and apoptosis escape. However, little is known about cellular miRNA deregulation during the development of GaHV-2-associated lymphoma. We determined the cellular miRNA expression profiles of chickens infected with a very virulent strain (RB-1B) or a vaccine strain (CVI988) or noninfected. Among the most deregulated cellular miRNAs, we focused our efforts on gga-miR-21, which is upregulated during GaHV-2 infection. We mapped the gga-miR-21 promoter to the 10th intron of the *TMEM49* gene and found it to be driven by AP-1- and Ets-responsive elements. We show here that the viral oncoprotein Meq binds to this promoter, thereby transactivating gga-miR-21 expression. We confirmed that this miRNA targets chicken programmed death cell 4 (PDCD4) and promotes tumor cell growth and apoptosis escape. Finally, gga-miR-21 was overexpressed only during infection with a very virulent strain (RB-1B) and not during infection with a nononcogenic strain (CVI988), providing further evidence for its role in GaHV-2 lymphomagenesis. Our data therefore suggest an additional role for Meq in GaHV-2-mediated lymphomagenesis through the induction of miR-21 expression.**

Gallid herpesvirus 2 (GaHV-2) is a highly oncogenic chicken alphaherpesvirus that induces a T-cell lymphoma coined Marek's disease (MD) a few weeks after infection. In addition to being a major burden for the poultry industry, GaHV-2 is considered an excellent model of virus-induced lymphoma (1). Its genomic organization is similar to that of herpes simplex virus 1 in the unique long ($U_L$) and unique short ($U_S$) regions (2, 3), whereas the long repeat ($R_L$) and short repeat ($R_S$) regions harbor specific genes involved in latency, lymphomagenesis, and transformation. One of these genes, *meq* (Marek EcoRI Q fragment), which is expressed in all GaHV-2 tumors and latently infected cells, encodes a 339-amino-acid protein and is considered the major oncogene of GaHV-2 (4). Meq has a basic leucine zipper (bZIP) structure at its N-terminal end similar to that of other bZIP proteins of the Jun/Fos family and a proline-rich region (PRR) in the C-terminal transactivator domain (4, 5). Several studies have shown that Meq can form either heterodimers with other bZIP proteins, such as c-Jun, that bind to AP-1-responsive elements (REs), such as CRE (TGACGTCA) or TRE (TGASTCA), or homodimers that bind to Meq-responsive element II (MEREII) (RACACACAY) and with a lower affinity to MEREI (GAGTGATGACGTCATC) (5, 6). The transactivation properties of Meq depend on its dimerization partner: Meq/Meq homodimers repress expression of the pp24/38 gene by binding to a MEREII site (6), whereas Jun/Meq heterodimers transactivate the expression of *ICP4* and *meq* by binding to AP-1 REs (6–8). Meq may also regulate cellular genes, such as those for interleukin-2 (IL-2) (6), CD30 (1), and Bcl-2 (7), and may increase the transcription of genes involved in growth and antiapoptotic pathways, such as the Jun pathways, during the induction of MD virus (MDV) lymphomagenesis (9).

The viral microRNAs (miRNAs) encoded by GaHV-2 were first identified in 2006 by Burnside et al. (10). Additional studies completed the identification of these viral miRNAs, and 26 mature miRNAs have now been described (MiRBase release 18, November 2011). GaHV-2 miRNAs are localized in the $R_L$ and $R_S$ regions and are grouped into three clusters, one upstream and one downstream from the *meq* gene (mdv1-miR-M9-M4 and -M11-1, respectively) and one at the 5′ end of the latency-associated transcript (LAT; mdv1-miR-M8-M10) (11). Different expression patterns have been reported for these miRNAs, but high levels of mdv1 miRNA seem to be associated with latency and tumorigenesis (10, 12, 13), suggesting a potential role for these miRNAs in the control of apoptosis and cell proliferation. Indeed, mdv1-miR-M4-5p has been characterized as a functional ortholog of the oncogenic miR-155 and is thought to be involved in lymphoid malignancy, immune response regulation, or viral cycle control (14, 15). A critical role for mdv1-miR-M4 in MDV lymphomagenesis has been demonstrated (16). In addition, it has recently been reported that another miRNA, mdv1-miR-M3, significantly decreases cisplatin-induced apoptosis in DF1 cells, by targeting *smad2* and the transforming growth factor β signaling pathway (17). It is now also widely accepted that viral infection and tumorigenesis are linked with disruption of the cellular miRNA profile.

**Received** 10 September 2012 **Accepted** 2 October 2012

**Published ahead of print** 10 October 2012

Address correspondence to Denis Rasschaert denis.rasschaert@univ-tours.fr.

Supplemental material for this article may be found at http://dx.doi.org/10.1128/JVI.02449-12.



doi:10.1128/JVI.02449-12

An upregulation of miR-155 has classically been reported in various lymphomas (18, 19). Interestingly, miR-155 is repressed during GaHV-2 lymphomagenesis, but the virus compensated for its absence by expressing the viral ortholog mdv1-miR-M4-5p (14, 15, 20, 21). miR-221 and miR-222, upregulated in the MSB-1 cell line, have been shown to promote cell division (22). The deregulation of other miRNAs, such as miR-34, let-7, miR-150, the miR-17-92 cluster, and miR-21, can be observed in various tumors, but so far, only miR-21 has been found to be systematically overexpressed in human cancers, making it an ideal candidate for tumor diagnosis (23). The miR-21 promoter has been studied in humans, and its activity is regulated by transcription factors, such as AP-1, STAT3, and FoxO3a (24–26). MiR-21 has been characterized as an oncogene targeting several tumor suppressor genes, including phosphatase and tensin homolog (PTEN) and programmed death cell 4 (PDCD4), or regulating genes involved in cell invasion, such as the genes encoding matrix metalloprotease 2 (MMP2) and MMP9 (27, 28).

In this study, we found that gga-miR-21 was overexpressed during GaHV-2 infection and induced lymphomagenesis. We identified and characterized a robust promoter with a transcription initiation site. We found that the viral oncoprotein Meq bound to and transactivated gga-miR-21 via AP-1 response elements. gga-miR-21 may play a role in tumor growth and apoptosis inhibition, notably, by targeting PDCD4. Finally, the analysis of cellular miRNA profiles by small RNA cloning and deep sequencing showed that gga-miR-21 overexpression was specifically associated with oncogenic RB-1B strain infection and not with infection with the vaccine strain CVI988, providing further support for an oncogenic role of gga-miR-21.

## MATERIALS AND METHODS

**Virus strains and cell cultures.** The very virulent RB-1B strain used in this study was prepared from a stock of peripheral blood leukocytes (PBLs) collected from $B^{13}/B^{13}$ chickens at 42 days postinfection (dpi) that contained 1,000 PFU of cell-associated RB-1B virus. CVI988 (Poulvac batch MC97600 and MC18800) vaccines were obtained from Pfizer Animal Health (Belgium).

In this study, we used MSB-1 cells, which are latently infected and have the GaHV-2 genome integrated into their cellular genome. The MSB-1 cell line was one of the first GaHV-2-infected cell lines to be isolated (29) and is derived from a spleen lymphoma induced by a virulent strain of GaHV-2. It is currently widely used as a reference. It has been shown to be coinfected with GaHV-2 (strain BC-1) and GaHV-3 (strain HPRS24) (30). The cells were harvested at a density of $2 \times 10^6$ cells per ml. This cell line was cultured in RPMI 1640 medium (Lonza) supplemented with 1 mM sodium pyruvate, 10% fetal bovine serum, and 5% chicken serum. The lymphoblastoid B-cell line DT-40 (31) was obtained from a tumor induced by Rous-associated virus 1 (RAV-1) infection. It was cultured in Dulbecco modified Eagle medium (Lonza) supplemented with 1 mM sodium pyruvate and tryptose phosphate broth (1.475 g/liter) and with 10% fetal bovine serum and 5% chicken serum. DNA from the JBJ-1 (ATCC CRL-12203) and PA9 (32) cell lines was used to amplify the miR-21 promoter and the PDCD4 3′ untranslated region (UTR), respectively.

**Animal experiments.** We used 4-week-old White Leghorn $B^{13}/B^{13}$ chickens hatched and raised at INRA (PFIE-PlateForme d'Expérimentation Animale, Nouzilly, France) under specific-pathogen-free (SPF) conditions. This chicken line is highly susceptible to Marek's disease following experimental inoculation with virulent GaHV-2 strains.

Two successive experiments were carried out for reverse transcription-quantitative PCR (RT-qPCR) and the deep sequencing of small RNAs. Chickens were inoculated by the intramuscular route with $5 \times 10^6$ PBLs from a stock collected from a $B^{13}/B^{13}$ chicken at 42 dpi. The inoculum contained 1,000 PFU. We collected blood samples from three animals at 7, 21, and 28 dpi for RT-qPCR and from three animals at 0 and 27 or 29 dpi for the establishment of libraries of small RNA from chickens infected with strain RB-1B or CVI988. All the chickens were anesthetized and euthanized before necropsies were performed to check for MD. All RB-1B-infected chickens used in this study showed MD lymphoma development. All animal procedures were conducted in accordance with the guidelines of the INRA Ethical Commission (protocol numbers MD-2005-01A/-02A and GD.01.10B).

**Isolation of PBLs.** PBLs were separated from whole-blood samples by centrifugation on Ficoll-Hypaque (FH) cushions, as previously described (33). The cells were resuspended in RPMI 1640 medium and counted in a hemacytometer before RNA extraction.

**Generation and sequencing of small RNA libraries.** Total RNA was isolated by guanidinium thiocyanate-phenol-chloroform extraction (TRIzol; Invitrogen). Small RNAs were cloned from 30 μg of total RNA, as previously described (34), except that PCR products were not concatenated and were instead sent directly for large-scale sequencing. Small RNA molecules were sequenced at the Institut de Génétique et de Biologie Moléculaire et Cellulaire (IGBMC), Illkirch, France, on an Illumina Genome Analyzer Ilx instrument with a read length of 36 bp.

**Bioinformatic analysis.** An in-house Perl analysis pipeline was used to analyze the large amount of data generated. The 3′ adaptor was removed, and size selection was carried out (with the exclusion of trimmed reads of less than 15 nucleotides [nt]). Nonredundant sequences were then mapped to the genomes from which they were thought to be derived and to other already annotated RNAs with the Nexalign program (http://genome.gsc.riken.jp/osc/english/software/src/nexalign-1.3.5.tgz), with no mismatch allowed. The *Gallus gallus* and GaHV-2 genome sequences were downloaded from the RefSeq or GenBank database (Genome Assembly, version 2.1 [ftp://ftp.ncbi.nih.gov/genomes/Gallus_gallus/Assembled_chromosomes] and GenBank accession number EF523390.1). The following sources of annotated transcripts were used: miRBase version 16 for miRNA; GenBank version 181 for *Gallus gallus* rRNA, small nuclear-small nucleolar RNA (sn-snoRNA), and small cytoplasmic RNA (scRNA); Genome Assembly version 2.1 for tRNA; and Repbase version 181 for *Gallus gallus* and common ancestral repeats. Small RNAs mapping unambiguously to sequences from a single functional category were easily classified, whereas the others were identified by applying the following annotation rule on the basis of the abundances of various types of sequences in the cell: rRNA > tRNA > sn-snoRNA > miRNA > repeat > pathogen genome > host genome > unknown.

**Plasmid constructs.** The entire sequence of the putative promoter of gga-miR-21, extending from nucleotide 7,318,351 to nucleotide 7,318,796, was amplified from genomic DNA of the chicken cell line JBJ-1 (primers A140 and A141; Table 1). Various primers were used for directed mutagenesis by PCR (Table 1; see Fig. 3). PCR was performed as follows: heating at 94°C for 5 min, followed by 25 cycles of denaturation (94°C for 30 s), annealing (55°C for 30 s), and extension (72°C for 1 min) in a final volume of 50 μl containing 2.5 units of *Taq* DNA polymerase (Promega), 0.1 μM each primer (Eurogentec), 0.2 mM each deoxyribonucleotide, 10 mM Tris-HCl, pH 9, 50 mM KCl, 0.5 mM $MgCl_2$, 0.1% Triton X-100, and 50 ng DNA. All the putative promoter sequences were amplified with primer pairs (Table 1) with KpnI and HindIII sites in their tails. The KpnI/HindIII-digested PCR products were inserted, in the correct orientation, between the KpnI and HindIII sites of the pGL3basic vector (Promega).

Meq-RB-1B, Meq-CVI988, and Jun cDNAs were amplified from the bacmid RB-1B, CVI988 vaccine, and PA-9 cell genomes with specific primers with an EcoRI site in their tails (Table 1). The insertion of the PCR products in the correct orientation was checked by PCR, and sequencing (MWG) was performed to check the integrity of the DNA sequence.

**Luciferase assays.** The pGL3basic (Promega) expression vector was used to test the strength of promoters inserted upstream from the firefly luciferase (F-Luc) gene. The pRL-TK (Promega) vector includes an expression cassette

**TABLE 1** Primers used to construct promoter sequences and for ChIP, RACE-PCR, and RT-qPCR

| Primer orientation[a]-name | Sequence (5′–3′)[b] |
|---|---|
| F-A140-p21 | GTCA**GGTACC**AGCTCCGAAAACCTCATCAATCTTT |
| R-A141-p21 | AGTC**AAGCTT**CAGCCAGGGCTGTGTGCTG |
| F-A142-mutAP1-2 | GGATAAGGATAACACCCAGATTG |
| R-A143-mutAP1-2 | ATCTGGGTGTTATCCTTATCCAG |
| F-A144-mutAP1-4 | CACAAGCACAAACCCTTTCCTT |
| R-A145-mutAP1-4 | AGGAAAGGGTTTGTGCTTGTGT |
| F-A146-mutMERE | GACTAAGCTTCAGCCAGGGCAGAGAGCTGATGCG |
| R-A390-mutAP1-0 | CCCTGTTCAAAAAAATTTCATGCTTTATGGC |
| F-A391-mutAP1-0 | GCATGAAATTTTTTTGAACAGGGTTCATAG |
| R-A382-mutAP1-3 | TGACTTGTGCTAAAAAAATCCCTCAGTTAAAA |
| F-A383-mutAP1-3 | TAACTGAGGGATTTTTTTAGCACAAGTCATTTCC |
| R-A384-mutAP1-3-4-mutEts2 | GACTTGTGCTAAAAAAAAAAAAAAGTTAAAAAAG |
| F-A385-mutAP1-3-4-mutEts2 | CTTTTTTTTTTTTTTAGCACAAACCCTTTCC |
| R-A386-mutAP1-3-4 | GGGTTTGTGCTAAAAAAATCCCTCAGTTAAAAAAG |
| F-A387-mutAP1-3-4 | AACTGAGGGATTTTTTTAGCACAAACCCTTTCC |
| R-A388-mutAP1-1 | CCCATCGGAAAAAAATTAACAAAGGAACAA |
| F-A389-mutAP1-1 | TTTGTTAATTTTTTTCCGATGGGAGGAGC |
| R-A331-mutEts-3 | CACCAGCAGTTTTTGTAAGAACTGGTTTGAACCG |
| F-A330-mutEts-3 | AGTTCTTACATTTTCTGCTGGTGATAAATGTGGG |
| R-A329-mutEts-2 | TTGTGTCAAAAAAAAGTTAAAAAAGAAACTGCTCGCCC |
| F-A328-mutEts-2 | TTAACTTTTTTTTGACACAAGCACAAGTCATTTCC |
| R-A327-mutEts-1 | GTGCGTCATTTTTTTTTAGAAAGAATGCATTAGC |
| F-A326-mutEts-1 | CTTTCTTTTTTTTTATGACGCACAGATTGTCC |
| F-A341-mutAP1-4-mutEts-2 | TTAACTTTTTTTTGACACAAGCACAAACCCTTTCC |
| R-A340-mutAP1-2-mutEts-1 | GGGTGTTATAAAAAAAAAGAAAGAATGCATTAGC |
| F-A339-mutAP1-2-mutEts-1 | CTTTCTTTTTTTTTATAACACCCAGATTGTCC |
| GeneRacer-RNA oligonucleotide | CGACUGGAGCACGAGGACACUGACAUGGACUGAAGGAGUAGAAA |
| F-GeneRacer 5′ oligonucleotide | CGACTGGAGCACGAGGACACTGA |
| F-GeneRacer 5′ nested oligonucleotide | GGACACTGACATGGACTGAAGGAGTA |
| R-A233-GeneRacer-miR21 | AGAAGGCTCTGCTGCTTGGT |
| R-A234-GeneRecer nested-miR21 | CCCAGGGAGAAGGCAGAGCGA |
| qmiR-21-5p | CATGATCAGCTGGGCCAAGATCAACATCAGT |
| UP-qPCRmiR-universal primer | CATGATCAGCTGGGCCAAGA |
| UP-AS-U6 | CATGATCAGCTCGGCCAAGAGAACGCTTCAC |
| LNA-miR-21-5p | TEGLTZATCAGACTGAT |
| qPCR-U6 | CGCAAGGATGACACGCAAA |
| UP-ASmiR-21-5p | CATGATCAGCTGGGCCAAGATCAACATCAGTCTGATAAGCTA |
| F-A815-pmeq | GCTGGAAAACCATCGTAGAAC |
| R-A816-pmeq | CGTATCACTCCCGAACCATTA |
| F-A373-UL26 | TTGCACAGTCGGAGCAGTTCTTGCGC |
| R-A374-UL26 | TGACTGGCGGCTGTCTCTAGTGTACG |
| F-595-pp38 | TCTCCCTCTCCGGTTAGCTC |
| R-658-pp38 | ATGGAATTCGAAGCAGAACACGAAGGG |
| F-M450-Gapdh | TCCTCTCTGGCAAAGTCCAAG |
| R-451-Gapdh | CACAACATACTCAGCACCTGC |
| F-818-Meq | CACCCCTTCCCTGACGGCCTATC |
| R-820-Meq | CTCGAATTTCCTTACGTAGGTG |
| F-A406-PDCD4 | **GCGGCCGC**GTTGGAACCAACTGCTGAAG |
| R-A422-PDCD4 | **GCGGCCGC**GTACGTGCTGGCTGAAC |
| F-A420-PDCD4mut | GCCTTCACTACCATGACCTTTTGTAAGTGCCATA |
| R-A421-PDCD4mut | CAAAAGGTCATGGTAGTGAAGGCACCGCCACAACAG |
| F-A378-cJun | **GAATTC**ATGGAGCCTACTTTCTACG |
| R-A377-cJun | **GAATTC**TCAAACGTTTGCAACTG |
| F-M580-Meq | ATGTCTCAGGAGCCAGAGCCGGGCGCT |
| R-M581-Meq | GGGGCATAGACGATGTGCTGCTGAG |

[a] F, forward; R, reverse.
[b] KpnI, HindIII, NotI, and EcoRI restriction sites are shown in bold typeface. Mutated bases are underlined.

for *Renilla* luciferase (R-Luc) under the control of the thymidine kinase promoter of human herpesvirus 1 (HHV-1). Cotransfection with these two vectors (pGL3 carrying the test promoter and pRL-TK) made it possible to normalize measurements for transfection efficiency.

DT-40 and MSB-1 lymphoblastoid cells were transfected with plasmids by electroporation with an Amaxa Biosystems Nucleofector machine. The cell density was adjusted to $2 \times 10^6$ cells/100 μl of Nucleofection T solution containing 2 μg of the firefly luciferase reporter construct

and 40 ng of the *Renilla* luciferase control vector. The cells were then electroporated in a 4-mm cuvette subjected to the specific programs X-001 and B-023 for MSB-1 and DT-40, respectively. For luciferase assays with the expression vector pcDNA-Meq or Jun, 1 μg of each firefly promoter construct was mixed with 2 μg of the induction vector pcDNA and 40 ng of the reporter vector pRL-TK. Electroporated cells were recovered in 1.5 ml of complete medium and dispensed into a 12-well plate. The functionality of gga-miR-21 was assessed in DT-40 cells by the same method with 1 μg of each target *Renilla* reporter vector (pRL-TK-target) and 200 ng of pcDNA-Mluc, to standardize for transfection efficiency.

Luciferase assays were performed 24 h after transfection with a dual luciferase reporter assay system (Promega) and a Centro LB960 luminometer (Berthold Technologies). Student's *t* test (performed with GraphPad Prism software 4) was used for statistical analysis.

**5′ RACE-PCR analysis.** 5′ rapid amplification of cDNA ends (5′ RACE) was carried out on total RNA isolated from MSB-1 cells. Total RNA was extracted with a TRIzol extraction kit. cDNAs were obtained with a GeneRacer kit (Invitrogen). This technique is based on RNA ligase-mediated and oligonucleotide-capping RACE methods and results in the selective ligation of an RNA oligonucleotide to the 5′ ends of decapped RNA. The resulting cDNA was amplified by PCR, using forward primers annealing to the ligated RNA oligonucleotide and reverse primers annealing to the target gene (Table 1).

The 5′ end of the ligated cDNA obtained from MSB-1 cells was determined with a reverse primer binding to the potential miRNA sequence (Table 1). PCR products of various sizes were obtained and inserted into the PCR4-TOPO TA cloning vector. We sequenced 32 positive clones and determined the 5′ end in each case.

**ChIP assays.** Chromatin immunoprecipitation (ChIP) assays were carried out as previously described (35). Briefly, chromatin from $10^7$ MSB-1 cells was cross-linked, washed, resuspended in lysis buffer, and sonicated with 12 6-s 18-J pulses (VibraCell Bioblock Scientific). An aliquot of total chromatin was used as the total DNA input control. After preclearing with protein G agarose/salmon sperm DNA beads, protein/DNA complexes were immunoprecipitated by incubation overnight at 4°C with anti-Meq (36 μl of polyclonal rabbit antibody obtained in our laboratory) or anti-Jun (4.5 μl of purified polyclonal rabbit antibody; 06#225; Upstate) antibody or with mouse immunoglobulin G1κ (6 μg of IgG1κ; Sigma-Aldrich) as a negative control. Immunoprecipitated complexes were collected with protein G beads. Immunoprecipitation products were washed with low-salinity buffer, high-salinity buffer, lithium chloride washing buffer, and, finally, TE (Tris-EDTA) buffer. Immunocomplexes were extracted, and cross-linking was reversed by incubation overnight at 65°C. DNA fragments were then purified with a Nucleospin Extract II apparatus (Macherey-Nagel) and eluted in 30 μl of ultrapure water. PCR was performed in a final volume of 50 μl with Promega *Taq* DNA polymerase and primer pairs A140/A141, A815/A816, and A373/A374 (Table 1). PCR was carried out as follows: heating at 94°C for 3 min at 94°C, followed by 22 cycles of 94°C for 45 s, 55°C for 45 s, and 72°C for 1 min and, finally, 7 min at 72°C.

**Western blot analysis.** We treated $5 \times 10^5$ MSB-1 cells or transfected DT-40 cells with lysis buffer (15 mM Tris, 15 mM NaCl, 20 mM EDTA, 1% SDS, 5% beta-mercaptoethanol, 20% glycerol, bromophenol blue [pH 6.8]). Proteins were separated by electrophoresis in 10% polyacrylamide gels containing SDS and capillary transferred onto nitrocellulose membranes. The membranes were blocked by incubation with blocking buffer (Odyssey) and probed with polyclonal rabbit anti-Meq (from our laboratory) or anti-PDCD4 (ab31392; Abcam) antibodies or monoclonal mouse anti-Jun (1/500e; BD Sciences) or mouse anti-GAPDH (glyceraldehyde-3-phosphate dehydrogenase; Millipore) primary antibodies, followed by monoclonal goat anti-rabbit or anti-mouse infrared dye (IRD)-labeled secondary antibodies (Odyssey). The immunoreactions of interest were detected after excitation with light at wavelengths of 700 nm and 800 nm for antimouse and antirabbit antibodies, respectively.

**Detection of RNA expression by RT-PCR.** Total RNA was isolated by guanidinium thiocyanate-phenol-chloroform extraction (TRIzol; Invitrogen) and quantified with Qbit methods. We then synthesized cDNAs in random primer and oligo(dT) primer extension assays with 1 μg of total RNA. After reverse transcription, PCR was performed on 1 μl of cDNA in a reaction volume of 50 μl with Promega *Taq* DNA polymerase and specific primers (Table 1). PCR was carried out as follows: heating at 94°C for 3 min, followed by 30 cycles of 94°C for 30 s, 55°C for 30 s, and 72°C for 1 min and, finally, 7 min at 72°C.

**miRNA quantification by RT-qPCR.** gga-miR-21 RNA levels were determined as described by Raymond et al. (36). Briefly, total RNA was isolated by guanidinium thiocyanate-phenol-chloroform extraction (TRIzol; Invitrogen) and quantified with Qbit methods. We then synthesized cDNAs in specific primer extension assays with 1 μg of total RNA (Table 1). After reverse transcription, triplicate measurements were made on 5 μl of cDNA diluted 1 in 10 in a final reaction volume of 25 μl by qPCR in a 96-well optical PCR plate with a StepOneplus machine (Applied Biosystems) and a SYBR green PCR mixture containing 12.5 μl SYBR green PCR master mix (Applied Biosystems), 3.5 μl water, 1 μl of 10 μM universal primer, 2 μl of 10 μM primer LNA-miR-21-5p, and 5 μl of sample. The primer sequences are reported in Table 1. qPCR was carried out under the conditions recommended by the manufacturer, and postrun dissociation curves were generated for the analysis of amplicon species.

**Flow cytometry analysis.** We mixed $2 \times 10^6$ MSB-1 cells with 200 pmol of anti-miR-21 locked nucleic acid (LNA) antisense primer or with scramble primer (Table 1). Twenty-four hours after treatment, the cell density was adjusted to $1 \times 10^6$ cells/ml and the cells were mixed with staining buffer solution containing 10 μl of fluorescein isothiocyanate (FITC)-annexin V and propidium iodide, as recommended by the manufacturer (BD Sciences). We then analyzed $3 \times 10^5$ cells by flow cytometry (IASP cytometry platform; INRA Tours, Nouzilly, Yves Le Vern, France), using 530/540-nm and 540/620-nm band-pass filters for FITC and propidium iodide, respectively.

## RESULTS

**miRNA-21 is overexpressed during natural infection with GaHV-2.** Yao et al. found that gga-miR-21 was the most abundantly expressed cellular miRNA in GaHV-2-transformed MSB-1 cells (37), and we previously found this miRNA to be the fourth most abundantly expressed miRNA in this cell line (data not shown). We extended these observations by investigating gga-miR-21 expression during natural infection. Chickens were infected by the intramuscular injection of PBLs containing 1,000 PFU of the very virulent GaHV-2 RB-1B strain. Using RT-qPCR, we quantified gga-miR-21 expression in total RNA extracted from PBLs from three chickens before infection and 7, 21, and 28 dpi (Fig. 1A). For the 3 chickens, the level of miR-21 expression increased significantly ($P < 0.05$) from 7 dpi onward. At 21 dpi, a time point corresponding to the implementation of lymphomagenesis in our *in vivo* model (38), the level of miR-21 expression was up two times compared to its level of expression before infection. Expression of viral *meq* and *pp38* genes during infection was assessed by RT-PCR, and amplicons were found, as expected (Fig. 1B).

**gga-miR-21 is transactivated from a well-conserved sequence located 3.3 kb upstream from the pre-miRNA sequence.** Given the fact that the expression of gga-miR-21 seemed to be induced in chicken PBLs during *in vivo* infection with a virulent strain of GaHV-2, we investigated the promoter driving miR-21 expression in the context of Marek's disease. A recent study identified the promoter of human miR-21 (hsa-miR-21) within a 454-bp sequence mapping to the 10th intron of the *TMEM49* gene

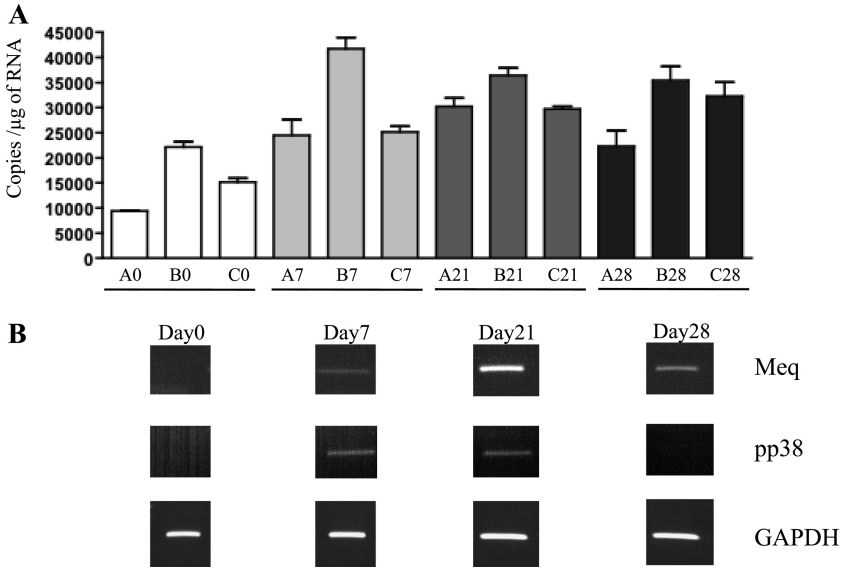


**FIG 1** Expression of microRNA-21 during GaHV-2 infection *in vivo.* Three chickens (chickens A to C) were infected with the very virulent RB-1B strain of GaHV-2. PBLs were collected at 0, 7, 21, and 28 days after infection, and RNA was extracted with the TRIzol reagent. (A) RT-qPCR was performed with an Applied Biosystems analysis kit to assess gga-miR-21 expression. Each value corresponds to the mean of three replicates for RNA extracted from the blood of one chicken. The error bars correspond to the SEMs. (B) RT-PCR was performed on pooled cDNA to confirm expression of viral genes during infection.

on chromosome 17 (24). The alignment of this human sequence with the homologous 446-bp avian sequence located in the 10th intron of the *TMEM49* gene (chromosome 19, coordinates 7,318,351 to 7,318,796) showed that the two sequences were 79.4% identical (see Fig. S1 in the supplemental material). *In silico* analysis with the Genomatix software suite led to the identification of several potential responsive elements (REs), including one TATA box, five AP-1 sites, three Ets/PU.1 sites, two CEBPβ sites, two STAT3 sites, and one GC box. Almost all the REs were conserved in humans and chickens, but the potential AP-1(0) RE and the MEq response element (MERE) were specific to the chicken promoter (see Fig. S1 in the supplemental material).

We assessed the functionality of this putative promoter by mapping the transcription start site (TSS) involved in gga-pri-miR-21 transcription. To this end, we performed a rapid amplification of 5′ cDNA ends (RACE) on total RNA extracted from MSB-1 cells, which are latently infected with GaHV-2. All of the 32 TSSs discovered mapped to a 107-bp region well conserved in the human and avian species (Fig. 2A and B; see Fig. S1 in the supplemental material). Of these TSSs, 91% (29 hits) localized to a 5-bp region (on chromosome 19, coordinates 7,318,753 to 7,318,758) and 62% (20 hits) were focused on nt 7,318,758 (Fig. 2C). This region, which is well conserved in humans, was thus identified as the probable promoter of the gga-pri-miR-21 transcript. We then looked for mechanisms regulating the transcriptional activity of this region.

**The pri-miRNA-21 promoter contains numerous consensus responsive elements and seems to be controlled by AP-1 and Ets transcription factors.** We investigated the mechanisms involved in transcriptional activity by amplifying by PCR from JBJ-1 chicken DNA the region extending from 407 nt upstream to 38 nt downstream of the major TSS (chromosome 19, coordinates 7,318,351 to 7,318,796) and inserting the amplicon into a promoterless luciferase reporter plasmid (pGL3basic) to generate the pmi21 wild-type (WT) construct. The pmi21 WT construct resulted in transcriptional activity similar to that of the cytomegalovirus promoter (data not shown). We therefore mutated all the REs for AP-1 and Ets, transcription factors known to be involved in lymphogenesis and lymphomagenesis. The AP-1 REs specifically bind dimers from the Jun/Fos family, including the GaHV-2 oncoprotein Meq, whereas MERE binds only the Meq oncoprotein as a homodimer and the Ets REs bind Ets family proteins, such as Ets-1, Ets-2, and PU.1. All the potential AP-1 and Ets REs identified by bioinformatics are degenerated with regard to the consensus sequences (Fig. 3B). We evaluated the potential role of these REs in promoter activity by mutating them individually by directed mutagenesis, based on overlapping PCR, and the resulting mutated promoter sequences were inserted into the pGL3basic vector to generate the A0*, A1*, A2*, A3*, A4*, MERE*, E1*, E2*, and E3* constructs, named according to their positions with respect to the 5′ end of the promoter (Fig. 3A). The promoter activities of these constructs were determined by the transfection of two avian cell lines, DT-40 and MSB-1, with all the constructs (Fig. 3C and D). In DT-40 cells, only MERE and Ets(1) RE mutations had no effect on transcriptional activity. In this cell line, mutations of the AP-1(0) RE and AP-1(3) REs increased promoter activity by factors of 1.7 and 2, respectively, whereas mutation of the other REs decreased promoter activity. Mutations of the AP-1(1) and AP-1(2) REs induced slight decreases (20%) in transcriptional activity, whereas the largest decreases in activity resulted from mutations of the AP-1(4), Ets(3), and Ets(2) REs, resulting in 50%, 50%, and 80% decreases, respectively (Fig. 3C).

In MSB-1 cells, in addition to the MERE and the Ets(1) REs already identified to be nonfunctional in DT-40 cells, the AP-1(0), AP-1(1), and AP-1(2) REs did not seem to be involved in promoter activity (Fig. 3D). Conversely, in this cell line, AP-1(4), Ets(2), and Ets(3) were found to be essential REs for the promoter, as their mutation resulted in a 2-fold reduction of transcriptional

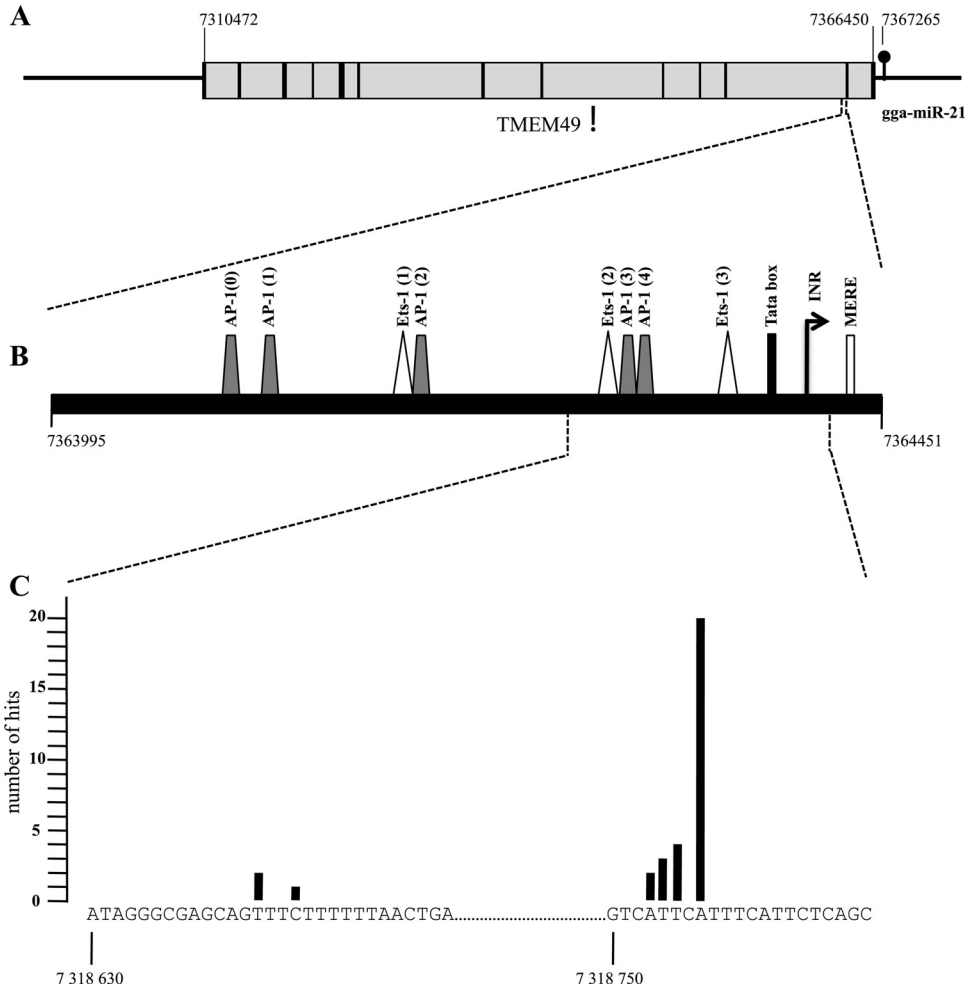


**FIG 2** Localization of the transcription start site of pri-miRNA-21. (A) Schematic diagram of a fragment of avian chromosome 19 encoding gga-miR-21 downstream from the *RTMEM49* gene. (B) Schematic diagram of the putative gga-miR-21 promoter, with potential responsive elements identified by the Genomatix software suite. (C) Localization and frequencies of the transcription start sites found by 5′ RACE-PCR in total RNA from MSB-1 cells. Each histogram shows the number of transcripts initiated from the nucleotide of the reference sequence (GenBank accession number NW_001471508.1).

activity (Fig. 3D). Mutation of the AP-1(3) RE decreased transcriptional activity by 20% in the MSB-1 cell line.

We evaluated the potential cooperation between the different REs by generating three constructs with multiple RE mutations [A(01234)*, E(123)*, and A(01234E123)*]. No significant decrease in promoter activity was observed with these promoters with multiple mutations, as shown by comparisons of activity for AP-1(4)* and Ets(2)*. This suggests that there is no cooperation between the various REs (Fig. 3) and that REs AP-1(4) and Ets(2) are both major REs of the gga-miR-21 promoter.

**Meq directly binds to and transactivates the promoter of gga-miR-21.** As Meq could bind to AP-1 REs as a heterodimer with Jun/Fos family proteins, including c-Jun, in particular, we investigated the efficiency of gga-miR-21 promoter transactivation by these proteins. We first checked that both c-Jun and Meq bound to the gga-miR-21 promoter by ChIP assays on DNA from MSB-1 cells (Fig. 4A), which constitutively express Meq (Fig. 4B). PCR with primers surrounding the gga-miR-21 promoter, the *meq* promoter (positive control) (6), and the $U_L26$ DNA fragment (negative control) was performed on Meq- and c-Jun-immunoprecipitated DNA. We could detect amplicons only for the *meq* promoter and the gga-miR-21 promoter (Fig. 4A), which indicated that both Meq and c-Jun proteins were effectively recruited by the gga-miR-21 promoter. We then ruled out possible effects of the virus present in the MSB-1 cells by determining the transactivation efficiency of c-Jun and Meq after ectopic production of these two proteins in uninfected DT-40 cells. DT-40 cells were cotransfected with pcDNA-Meq or pcDNA-Jun, encoding Meq and c-Jun, respectively, or an empty vector (pcDNA). We first verified the production of Meq by the pcDNA-Meq vector (Fig. 4B) and the overexpression of c-Jun by the pcDNA-Jun vector (Fig. 4C) (which was found to be by a factor of 2), validated by Western blotting (Fig. 4B and C). We then assessed the effect of these two constructs by cotransfecting them together with pmi21 WT or three constructs with multiple mutations in REs. As can be seen in Fig. 4D, Meq and Jun had similar effects on the different promoters: (i) Meq and Jun increased the promoter activity of pmi21 WT by factors of 2.4 and 2.5, respectively; (ii) AP-1 RE mutated constructs did not display any increase in

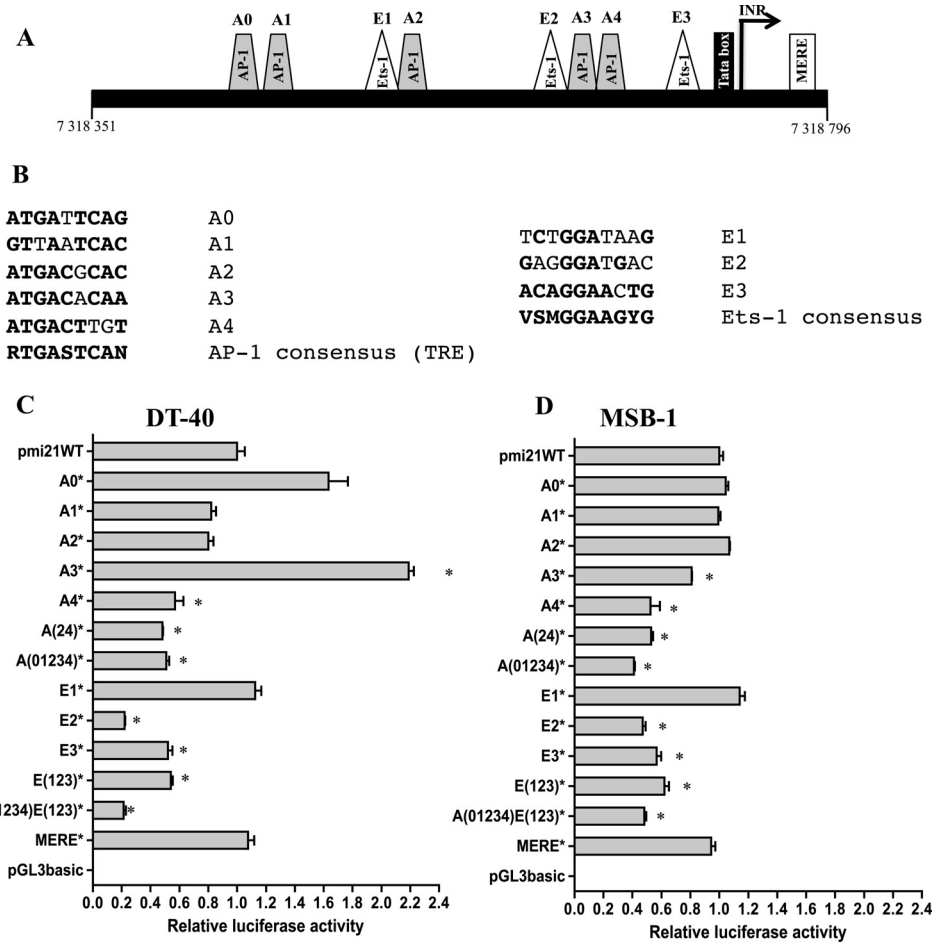


**FIG 3** Identification of the transcription factors involved in the transcriptional activity of the gga-miR-21 promoter. (A) Schematic diagram of the gga-miR-21 promoter with AP-1, Ets, TATA box, and INR elements. (B) Sequence alignments of the 5 AP-1 and the 3 Ets REs identified by bioinformatics, with nucleotides similar to the consensus sequence shown in bold. (C and D) The promoter activities of the various constructs (the REs mutated are indicated for each histogram) were assessed in the DT-40 (C) and MSB-1 (D) cell lines. Each reported luciferase activity value was normalized with respect to that of the pmi21 WT promoter construct. Each value corresponds to the mean of three independent assays performed simultaneously. Error bars indicate the SEMs of three replicates, and asterisks to the right of the bars indicate that the means are significantly different ($P < 0.01$) in comparison to the WT construct.

activity, showing that they were not transactivated by either of the proteins; and (iii) Ets RE mutated constructs displayed a 1.6 times increase in activity. Therefore, these data indicate that, like c-Jun, Meq may transactivate the gga-miR-21 promoter essentially by binding to AP-1 REs.

**gga-miR-21 downregulates chicken *PDCD4* expression and modulates MSB-1 tumor cell growth and apoptosis.** As hsa-miR-21 is considered to be an oncomiR regulating proapoptotic pathways by downregulating *PDCD4* expression (27), we investigated the possible targeting of the PDCD4 mRNA by gga-miR-21 in our chicken model. Using the custom program Targetscan (release 4.1), we predicted a potential gga-miR-21 target in the 5′ part of the chicken *PDCD4* 3′ UTR. Furthermore, alignment of the human and chicken *PDCD4* 3′ UTRs (GIs 27290 and 374191, respectively), which displayed a global identity of 63%, showed that both targets were located about 250 bp (276 bp and 233 bp, respectively) downstream from the start of the *PDCD4* 3′ UTRs at the 5′ end of a 100-bp more highly conserved region (82% identity). The full chicken *PDCD4* 3′ UTR sequence was amplified from the PA-9 cell genome and inserted into pRL-TK. The seed match of gga-miR-21 was mutated by PCR and inserted into the same vector (Fig. 5A). Following the transfection of DT-40 cells with these two constructs, relative luciferase activity was found to be twice as high when the putative miR-21 binding site was mutated (Fig. 5B). In addition, PDCD4 expression in pcDNA-miR-21-transfected MSB-1 cells was 25% lower than that in MSB-1 cells transfected with empty vector (Fig. 5C).

We also measured the regulation of PDCD4 by miR-21 in infected cells. To this end, we treated latently infected MSB-1 cells with 200 pmol of antisense miR-21-LNA. This resulted in a strong decrease (84%) in miR-21 accumulation (Fig. 6A) and a 2-fold increase in PDCD4 protein levels compared to the results for cells treated with a control scrambled LNA (Fig. 6B). To gain further insight into the effect of miR-21 inhibition, we assessed the impact of the anti-miR-21 LNA oligonucleotide on MSB-1 cell growth and apoptosis. We therefore counted cells and measured apoptosis by flow cytometry assays upon treatment with control anti-miR-21 oligonucleotides. The anti-miR-21 treatment inhibited the growth of the MSB-1 cells by 27% (Fig. 6C) and increased MSB-1 apoptosis by 20% and 24%

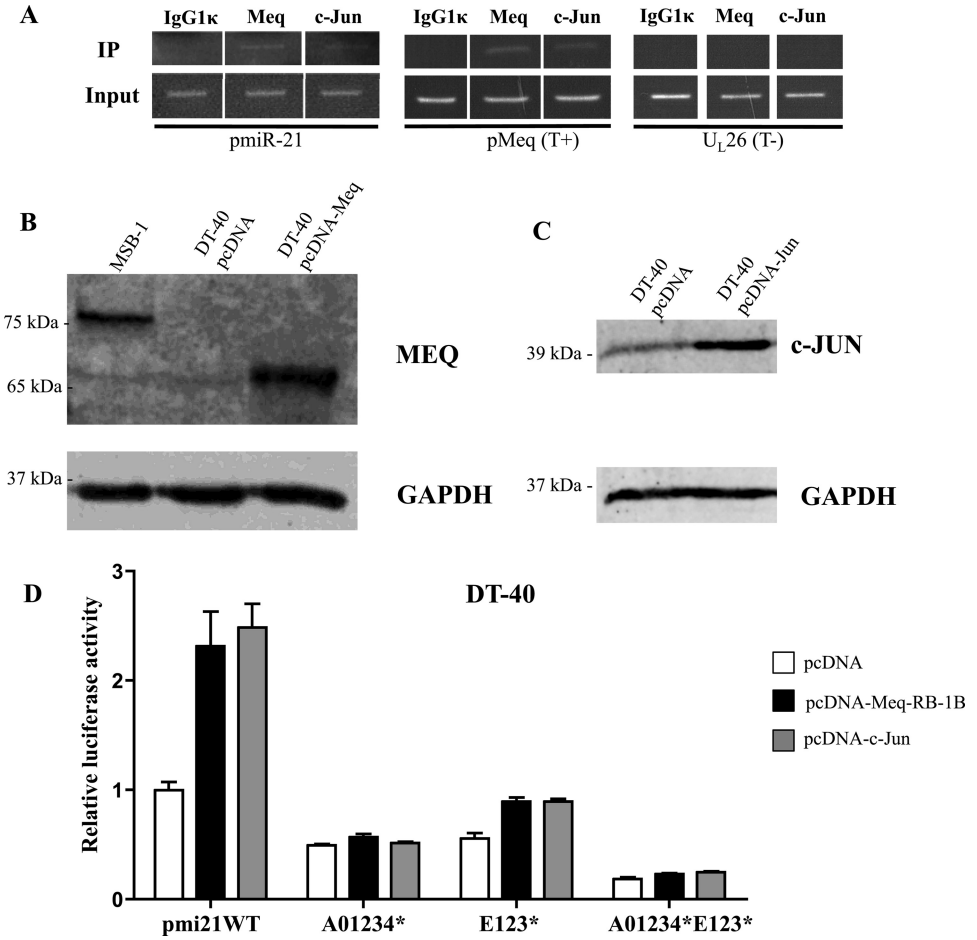


**FIG 4** Meq and c-Jun bind and transactivate the gga-miR-21 promoter. (A) Direct association of the Meq and Jun proteins with the gga-miR-21 promoter. PCR amplification was carried out with the F-A140-p21 and R-A141-p21 primers (Table 1). Electrophoretic analyses of the PCR amplification products obtained with immunoprecipitated DNA (IP) or total input DNA (Input) are shown. Mouse IgG1κ antibodies (left column) were used as a negative control in ChIP assays. The middle and right columns show the PCR amplification products for DNA immunoprecipitated with antibodies against Meq and Jun, respectively. (B and C) Western blot analysis of the ectopic production of Meq (B) or the overproduction of c-Jun (C). Each blot was probed with rabbit polyclonal anti-Meq or mouse monoclonal anti-Jun and mouse anti-GAPDH primary antibodies, followed by goat anti-rabbit or rabbit anti-mouse IRD-conjugated secondary antibody (Li-Cor). (D) Influence of c-Jun overproduction or of the ectopic production of Meq on the transcriptional activity of the gga-miR-21 promoter. Various gga-miR-21 promoter constructs were used to cotransfect DT-40 cells together with pcDNA encoding Meq, c-Jun, or an empty vector. Each reported luciferase activity value was normalized with respect to that of the pmi21 WT promoter construct used for cotransfection with the empty vector. Each value corresponds to the mean of three independent assays performed simultaneously. Error bars indicate the SEMs of three replicates.

in two independent assays, from 7.8% to 9.44% (Fig. 6D) and 6.12% to 7.58%, respectively, indicating a potential role for gga-miR-21 in modulating MSB-1 cell viability. However, several additional mechanisms should underlie the MSB-1 immortality.

**gga-miR-21 is specifically more strongly induced during infection with an oncogenic GaHV-2 strain than during infection with a vaccine strain.** Cellular miRNA profiles were analyzed in uninfected chickens, chickens infected with the oncogenic vvRB-1B GaHV-2 strain, and chickens infected with the nononcogenic vaccine strain CVI988 GaHV-2. Total RNA was extracted from PBLs collected from uninfected chickens or collected at 27 dpi from RB-1B GaHV-2-infected chickens and 29 dpi from CVI988 GaHV-2-infected chickens. From these PBLs, three libraries of small RNAs (PBL NI, PBL RB-1B D27, and PBL CVI988 D29, respectively) were constructed and analyzed by deep sequencing. We obtained 8 million to 14 million reads for the various small RNA libraries, and miRNAs accounted for 66 to 73% of all reads. All the sequences of cellular miRNAs can be accessed online (see Table S1 in the supplemental material). Expression ratios between infected and uninfected chickens were calculated for the 61 miRNAs detected at frequencies exceeding 0.1% in at least one of the three libraries (Table 2). We found that in the PBL RB-1B D27 and PBL CVI988 D29 libraries, respectively, 11 and 6 miRNAs were upregulated ($r > 2$), 31 and 48 were modulated only slightly, if at all ($2 \leq r \leq 0.5$), and 19 and 7 were downregulated ($r < 0.5$) (Table 2). Among these miRNAs, 8 were deregulated in both the PBL CVI988 D29 and PBL RB-1B D27 libraries (upregulated, miR-146c, -17-5p, and -19a; downregulated, miR-148a, -101, -92, -2954-5p, and -100) and 22 were deregulated only in the PBL RB-1B D27 library (upregulated, miR-21, -19b, -146c, -221, -2954-5p, 20b, -7b, and -144; downregulated, miR-181a, -30a-3p, -223, -126-3p, -1388, -1559, -182-5p, -99a-5p, -183, -1a-1, and -199-2-3p and let-7c and -7b) and could be considered potential

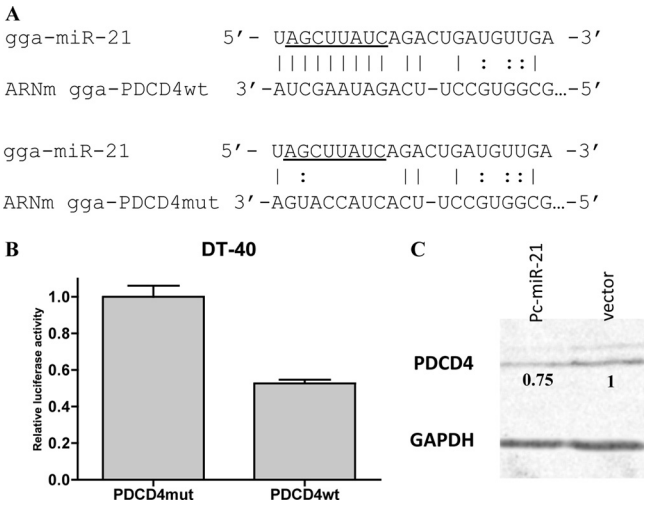


**FIG 5** Effect of the gga-miR-21 on PDCD4 expression. (A) Alignment of gga-miR-21 with the 3′ UTR PDCD4 WT or 3′ UTR PDCD4 mutant (PDCD4mut) mRNA targets. (B) Efficacy of endogenous gga-miR-21 with the PDCD4 3′ UTR bearing a single miRNA responsive element (miRE) carrying the predicted wild-type or mutant target. DT-40 cells were transfected with pRL-TK vector harboring a wild-type or mutant target and with pcDNA-Mluc for the standardization of transfection. Reporter activities were standardized by determining the ratio of *Renilla* to firefly luminescence. For each luciferase assay, relative luciferase activity was normalized with respect to the activity of the pRL-TK vector carrying the mutant target. Each value corresponds to the mean of three independent assays performed simultaneously. Error bars indicate the SEMs of three replicates. (C) Western blot analysis of PDCD4 levels after gga-miR-21 overexpression. MSB-1 cells were transfected with a pcDNA vector that was either empty or encoded gga-miR-21. Each blot was probed with rabbit anti-PDCD4 and mouse anti-GAPDH primary antibodies, followed by goat anti-rabbit or rabbit anti-mouse IRE dye-conjugated secondary antibody (Li-Cor). GAPDH was used as a control for equal protein loading. Relative signal intensities for PDCD4 were calculated with respect to the intensity for the GAPDH loading control with Adobe Photoshop element 6 software. The values indicated under the bands correspond to the level of PDCD4 relative to that detected in control cells.

markers of infection and lymphomagenesis, respectively. gga-miR-21 was one of the most strongly upregulated miRNAs at 27 dpi in the PBLs of chickens infected with the oncogenic RB-1B strain (2.4-fold induction), but no modulation (0.6-fold decrease) of its expression was observed at 29 dpi in chickens infected with the CVI988 strain (Table 2). In addition, we confirmed by RT-qPCR on these RNA samples that gga-miR-21 expression was increased (5.5-fold) in PBL RB-1B D27 and unmodulated in PBL CVI988 D29 (see Fig. S2 in the supplemental material). Interestingly, as previously described (38), Meq expression was undetectable in the PBL CVI988 D29 library of infection, in contrast to the PBL RB-1B D27 library (see Fig. S2 in the supplemental material). Thus, these *in vivo* data linking gga-miR-21 overexpression to the oncogenicity of the GaHV-2 strain highlight the potential role of gga-miR-21 in GaHV-2-induced lymphomagenesis.

In addition, the CVI988 Meq protein has three single nucleotide polymorphisms (SNPs) and isoforms with a 59-amino-acid insertion in the proline-rich domain (39, 40) affecting the transcriptional properties of the protein but not its AP-1-binding capacity (7, 41). We therefore compared the abilities of RB-1B and CVI988 Meq to transactivate the natural gga-miR-21 promoter. Empty vector and vectors encoding RB-1B Meq and CVI988 Meq (with the 3 SNPs already described [40]) were used to transfect DT-40 cells, and gga-miR-21 expression was then assessed by RT-qPCR. The transfection of cells with pcDNA-Meq-RB-1B increased gga-miR-21 expression by a factor of 4, whereas transfection with pcDNA-Meq-CVI988 increased gga-miR-21 expression by a factor of only 1.9 (Fig. 7).

## DISCUSSION

gga-miR-21 expression increased in parallel with GaHV-2 infection (Fig. 1) and associated lymphoma development. We define here, for the first time, the localization of TSS and the promoter of the pri-gga-miRNA-21 to the 10th intron of the *TMEM49* gene in the chicken genome. This 446-bp promoter is highly conserved in vertebrates (24), displaying 79.4% identity between humans and chickens. In chicken, the major TSS was found in a consensus initiator element (INR, YYANWYY) located 22 bp downstream from the TATA box shown to be functional in humans (24), consistent with the classical organization of class II promoters (42). Furthermore, the initiation start site beginning with the adenosine residue of the INR for more than half the transcripts is consistent with observations for TATA and INR promoters (43). The chicken miR-21 promoter was found to contain five degenerated AP-1 REs (TGASTCA) and three degenerated Ets REs. The Ets(2) and Ets(3) REs and the AP-1(4) RE, which are close to the TSS and the TATA box, seem to be essential in the both B- and T-cell lines. Besides the consensus sequence, this might explain their functionalities. Interestingly, several studies in humans have implicated the STAT3, Jun/Fos, and Ets protein families in the transcriptional functionality of the hsa-miR-21 promoter (25, 44), and the AP-1 RE equivalent to AP-1 (31) was found to be highly important (24). Furthermore, a recent study provided further evidence for AP-1 protein function, by demonstrating that curcumin, which prevents AP-1 protein binding to the hsa-miR-21 promoter, decreases hsa-miR-21 expression and inhibits tumor growth (45). AP-1 REs are frequently found in natural promoters, but they are not all functional. Conversely, several gene targets of Jun/Fos regulation harbor no AP-1 RE consensus sequences, and the dimerization partners of AP-1 proteins or other transcription factors may modulate expression of AP-1-dependent promoters (46). In MSB-1 cells, which are latently infected with GaHV-2, AP-1(4) seemed to be essential for promoter activity because a promoter in which this RE was mutated had a level of transcriptional activity similar to that of the promoter in which all the AP-1 REs were mutated (Fig. 3). Conversely, whereas mutations of AP-1(1) and AP-1(2) REs slightly decreased transcriptional activity in DT-40 cells and mutations of AP-1(3) increased this activity, no significant difference between the wild-type and mutated AP-1(1), AP-1(2), and AP-1(3) REs was observed in MSB-1 cells (Fig. 3). These differences in functionality between B cells (DT-40) and T cells latently infected and transformed with GaHV-2 (MSB-1) may be accounted for by the binding of different AP-1 protein dimers to the degenerated AP-1 REs, depending on the type of cell line (47). However, the doubling of transactivation observed in DT-40 when the AP-1(3) RE was mutated may result from allosteric modifications, facilitating the binding of Ets proteins to the closely adjacent RE Ets(2), shown to be functional in DT-40 cells (Fig. 3). These proteins seem to play an important role in promoter activity, because mutation of the Ets(2) RE decreased transcriptional activity by 75% in DT-40 cells and 50% in MSB-1 cells; this difference between B and T cells may be accounted for by the high levels of Ets family proteins, including PU.1, in particular, in B lymphocytes (48, 49).

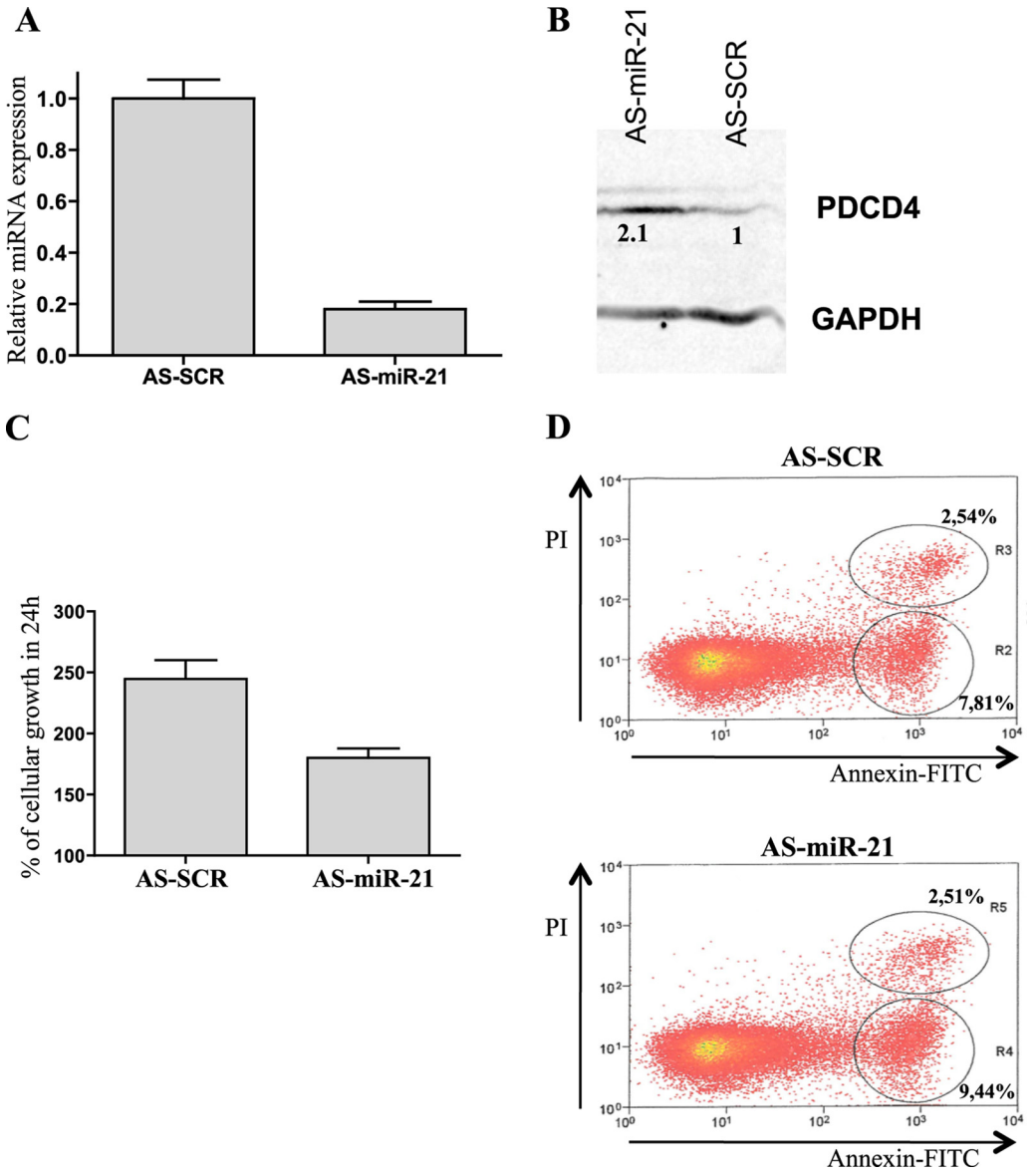


**FIG 6** Effect of antagomiR-21 treatment on PDCD4 expression, cell growth, and apoptosis in the MSB-1 tumor cell line. (A) Effect of the antagomiR-21 treatment of MSB-1 cells on gga-miR-21 expression. We treated $2 \times 10^6$ MSB-1 cells with 200 pmol of LNA AS-miR-21 or AS-SCR for 24 h. Total RNA was extracted, and RT-qPCR was performed to determine the levels of mature gga-miR-21. Each value was normalized with respect to that for U6 expression and is expressed relative to the level of gga-miR-21 in MSB-1 cells treated with scrambled LNA. Each value is the mean of three independent assays performed simultaneously. Error bars indicate the SEMs of three replicates. (B) Effect of the antagomiR-21 treatment of MSB-1 cells on PDCD4 expression. MSB-1 cells were treated with antagomiR-21, as previously described, and cells were harvested for the analysis of PDCD4 levels by Western blotting. Each blot was probed with rabbit anti-PDCD4 and mouse anti-GAPDH primary antibodies, followed by goat anti-rabbit or rabbit anti-mouse IRE dye-conjugated secondary antibody (Li-Cor). GAPDH was used as a control for equal protein loading. Relative signal intensities for PDCD4 were calculated with respect to the GAPDH loading control with Adobe Photoshop element 6 software. The values indicated under the bands indicate PDCD4 levels relative to those in control cells. (C) Effect of antagomiR-21 treatment of MSB-1 cells on cell growth. We used $2 \times 10^6$ MSB-1 cells to seed cultures, which were treated for 24 h with antagomiR-21 or scrambled LNA. The living cells were then counted. (D) Effect of gga-miR-21 on escape of MSB-1 cells from apoptosis. After antagomiR-21 treatment, the cells were labeled with FITC-annexin V and with propidium iodide (PI) solution for the detection of apoptotic and dead cells, respectively. We analyzed $3 \times 10^5$ cells from the R2 and R4 populations of cells treated with antisense miR-21 and with scrambled LNA, respectively. One representative experiment is presented.

Via its leucine zipper domain, Meq can form homodimers or heterodimers with other bZIP proteins of the Jun/Fos family (preferentially c-Jun). Both types of dimers are required for GaHV-2-induced T lymphomagenesis: the Meq/Meq homodimer as a transrepressor on MERE (MEq response element, ACACA) and the Meq/Jun heterodimer as a transactivator on the AP-1 RE (6, 8, 50–52). The predicted MERE repressor site, which, unlike the MERE of the pp14/38 promoter (6), is located just downstream from the TSS (see Fig. S1 in the supplemental material), did not seem to be functional (Fig. 3). Our data showing that the Meq protein can transactivate the gga-miR-21 promoter by binding to AP-1 REs, essentially AP-1(4) (Fig. 3, 4, and 7), provides evidence in favor of an oncogenic role of the viral protein Meq. This role in on-

**TABLE 2** Comparison of cellular miRNA signature from PBLs from uninfected chickens or chickens infected with RB-1B and CVI988 by deep sequencing[a]

| Sequence | miRbase | % of cellular miRNAs | | |
|---|---|---|---|---|
| | | Peripheral blood leukocyte | | |
| | | D27 RB-1B | D29 CVI-988 | Non Infected |
| TGAGGTAGTAGATTGTATAGTT | let-7f | 14,62 | 13,81 | 16,82 |
| TCAGTGCACTACAGAACTTTGT | miR-148a | 3,37 | 6,51 | 16,47 |
| TGAGGTAGTAGGTTGTATAGTT | let-7a/let-7j | 11,73 | 16,74 | 14,12 |
| CAACGGAATCCCAAAAGCAGCT | miR-191 | 13,87 | 17,63 | 8,35 |
| TAGCTTATCAGACTGATGTTGAC | miR-21 ← | 10,66 | 2,74 | 4,52 |
| TGAGGTAGTAGTTTGTGCTGTT | let-7i | 2,72 | 3,18 | 3,96 |
| TGAGAACTGAATTCCATGGACT | miR-146c | 15,19 | 7,19 | 3,17 |
| AACATTCAACGCTGTCGGTGAGT | miR-181a-5p | 0,93 | 2,68 | 3,05 |
| TGAGGTAGTAGATTGAATAGTT | let-7k | 2,69 | 1,66 | 2,06 |
| CATAAAGTAGAAAGCACTACT | miR-142-5p | 1,89 | 2,45 | 2,01 |
| TGAGGTAGTAGGTTGTATGGTT | let-7c | 0,43 | 2,04 | 1,94 |
| TTCAAGTAATCCAGGATAGGCT | miR-26a | 2,83 | 3,54 | 1,84 |
| TGTAAACATCCCCGACTGGAAG | miR-30d | 1,32 | 1,15 | 1,66 |
| GTACAGTACTGTGATAACTGA | miR-101 | 0,68 | 0,75 | 1,65 |
| AGCAGCATTGTACAGGGCTATGA | miR-103-2 | 2,37 | 1,97 | 1,62 |
| TATTGCACTTGTCCCGGCCTGT | miR-92 | 0,41 | 0,75 | 1,51 |
| **AATGACACGATCACTCCCGCTG** | **miR-425-5p** | 1,45 | 1,14 | 1,13 |
| GTAGTGTTTCCTACTTTATGGA | miR-142-3p | 0,65 | 0,99 | 1,09 |
| TACCACAGGGTAGAACCACGGA | miR-140-3p | 0,59 | 0,65 | 1,04 |
| CTTTCAGTCGGATGTTTACAGC | miR-30a-3p | 0,19 | 0,48 | 0,86 |
| TGTAAACATCCTTGACTGGAAGC | miR-30a-5p | 0,59 | 0,51 | 0,81 |
| TGTGCAAATCCATGCAAAACTGA | miR-19b | 1,39 | 1,00 | 0,57 |
| AACATTCATTGCTGTCGGTGGGT | miR-181b-1 | 0,28 | 0,35 | 0,56 |
| TGAGGTAGTAGTTTGTACAGTT | let-7g | 0,47 | 0,55 | 0,55 |
| CATCCCCATTCCACTCCTAGCAG | miR-2954 | 0,16 | 0,25 | 0,53 |
| TGTCAGTTTGTCAAATACCCCA | miR-223 | 0,13 | 0,53 | 0,53 |
| TAGCAGCACGTAAATATTGGTG | miR-16-1 | 0,56 | 0,60 | 0,49 |
| AACCCGTAGATCCGAACTTGT | miR-100 | 0,04 | 0,17 | 0,38 |
| TTAATGCTAATCGTGATAGGGGT | miR-155 | 0,46 | 0,50 | 0,35 |
| TGAGGTAGTAGGTTGTGTGGTT | let-7b | 0,15 | 0,56 | 0,35 |
| AATTGCACGGTATCCATCTGT | miR-363 | 0,66 | 0,16 | 0,34 |
| TCCCTGAGACCCTAACTTGTGA | miR-125b-5p | 0,06 | 0,28 | 0,33 |
| TCGTACCGTGAGTAATAATGCG | miR-126-3p | 0,11 | 0,37 | 0,28 |
| TGGGAGAGGATTGTTTACGCCT | miR-30c-1-3p | 0,20 | 0,26 | 0,24 |
| AGCTACATCTGGCTACTGGGTCTC | miR-222a | 0,44 | 0,22 | 0,24 |
| TGGCTCAGTTCAGCAGGAACAG | miR-24 | 0,32 | 0,29 | 0,21 |
| AAGCTGCCAGTTGAAGAACTGT | miR-22 | 0,22 | 0,21 | 0,21 |
| **ATCTCAGGTTCGTCAGCCCATG** | **miR-1388** | 0,05 | 0,32 | 0,20 |
| TAGCAGCACGTAAATACTGGAG | miR-16c | 0,23 | 0,26 | 0,19 |
| TTCGATGCTTGTATGCTACTCC | miR-1559 | 0,05 | 0,10 | 0,18 |
| **TTTGGCAATGGTAGAACTCACACT** | **miR-182-5p** | 0,07 | 0,10 | 0,17 |
| CAAAGTGCTTACAGTGCAGGTAG | miR-17-5p | 0,39 | 0,43 | 0,17 |
| AACCCGTAGATCCGATCTTGT | miR-99a-5p | 0,03 | 0,17 | 0,16 |
| TATGGCACTGGTAGAATTCACTG | miR-183 | 0,06 | 0,09 | 0,16 |
| TTCACAGTGGCTAAGTTCTGC | miR-27b | 0,09 | 0,18 | 0,16 |
| TGGAATGTAAAGAAGTATGTAT | miR-1a-1 | 0,02 | 0,16 | 0,15 |
| TCACAGTGAACCGGTCTCTTT | miR-128-2 | 0,18 | 0,31 | 0,15 |
| CAGGCTGGTTAGATGGTTGTC | miR-456 | 0,23 | 0,12 | 0,11 |
| AGCTACATTGTCTGCTGGGTTTC | miR-221 | 0,35 | 0,11 | 0,10 |
| TGTAAACATCCTACACTCTCAGCT | miR-30c-2 | 0,10 | 0,11 | 0,09 |
| ACAGTAGTCTGCACATTGGTT | miR-199-3p | 0,05 | 0,07 | 0,09 |
| **GCTGAGAGGGCTTGGGGAGAGGA** | **miR-2954-5p** | 0,19 | 0,08 | 0,08 |
| CAAAGTGCTCATAGTGCAGGTAG | miR-20b | 0,16 | 0,11 | 0,07 |
| CTAGTGATTTTTGTTGTT | miR-7b | 0,31 | 0,10 | 0,07 |
| TGAGAACTGAATTCCATAGGCG | miR-146b-5p | 0,06 | 0,10 | 0,07 |
| CAGTGGTTTTACCCTATGGTAG | miR-140 | 0,12 | 0,20 | 0,06 |
| TACAGTAGTCTGCACATTGGTT | miR-199-2-3p | 0,02 | 0,04 | 0,06 |
| ATCACATTGCCAGGGATTTCC | miR-23a-3p | 0,04 | 0,05 | 0,05 |
| TGAGATGAAGCACTGTAGCTC | miR-143-3p | 0,03 | 0,02 | 0,04 |
| TGTGCAAATCTATGCAAAACTGA | miR-19a | 0,46 | 0,45 | 0,03 |
| TACAGTATAGATGATGTACTC | miR-144 | 0,12 | 0,01 | 0,00 |

[a] Fold change in expression of cellular miRNAs in PBLs from uninfected chickens and chickens infected with RB-1B (PBLs collected at 27 dpi) or CVI988 (PBLs collected at 29 dpi). Cellular frequencies for each miRNA were estimated, and fold changes were calculated only for miRNAs with frequencies exceeding 0.1% in all three libraries. Overexpressed (green), unregulated (black), and downregulated (red) miRNAs were arbitrarily defined as having fold changes of expression of >2, between 0.5 and 2, and below 0.5, respectively. Newly identified miRNAs are in bold typeface.

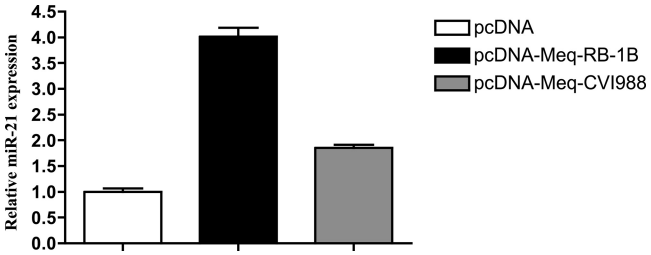


**FIG 7** Ectopic Meq production induces gga-miR-21 expression. DT-40 cells were transfected with vector pcDNA encoding RB-1B Meq or CVI988 Meq or with empty vector. The cells were harvested 24 h later; total RNA was extracted, and gga-miR-21 expression was assessed by RT-qPCR. Each value was normalized with respect to that of U6 expression and expressed relative to the level of gga-miR-21 in cells transfected with empty vector. Each value is the mean of three independent assays performed simultaneously. Error bars indicate the SEMs of three replicates.

comiR-21 overexpression can be added to the list of known interactions of Meq with the host cell: (i) interaction with C-terminal-binding protein (53), (ii) interference in Jun pathways (9), and (iii) activation of the cellular genes c-*ski*, *CD30*, *IL-2* and *Bcl-2* (1, 6, 7, 9, 52). Finally, although other deregulated microRNAs (miR-19b, miR-181a, let-7c, let-221) could be involved in oncogenesis (22, 54–57), comparative analysis based on data from the deep sequencing of small RNA libraries supports the role of gga-miR-21 in GaHV-2-induced lymphomagenesis. Indeed, gga-miR-21 overexpression was observed only in PBLs isolated from chickens infected with the oncogenic RB-1B strain and not in PBLs from those infected with the nononcogenic CVI988 strain (Table 2; see Fig. S2 in the supplemental material). CVI988 Meq seems to be a weaker transactivator of the gga-miR-21 promoter than RB-1B Meq (Fig. 7), as previously reported for several cellular and viral promoters (7, 41). However, we acknowledge that changes in the transactivating properties of CVI988 Meq may not be the only mechanism underlying the lower level of gga-miR-21 expression in CVI988-infected PBLs. The previously described lower level of Meq in PBLs (38), the lower viral replication (58), and other pathways may also be involved in gga-miR-21 regulation in the context of CVI988 infection.

A noteworthy fact is that two other lymphotropic herpesviruses, HHV-4 and HHV-8, induce hsa-miR-21 expression via the EBNA2 and K15 proteins, respectively (59, 60). This might contribute to the transformation properties of these two viruses. Similar mechanisms could be considered for GaHV-2 infection, because the viral protein Meq induced the expression of gga-miR-21, which seemed to target the chicken *PDCD4* gene, involved in apoptosis pathways (Fig. 5 and 6), as previously described in humans (61). As MSB-1 cells naturally express a high level of gga-miR-21 (37), pri-miR-21 transfection of MSB-1 cells only moderately modified PDCD4 expression (Fig. 6A), while the use of antagomiR-21 induced a marked difference of PDCD4 expression (Fig. 6B), supporting the involvement of gga-miR-21 in PDCD4 regulation. This slight regulation, as previously reported for anti-miR-21 treatment in human papillomavirus-positive cells (62) and for anti-miR-34a treatment in HCT cells (63), may contribute to the escape from apoptosis and growth of MSB-1 tumor cells (Fig. 6). Furthermore, a miR-21–PDCD4–AP-1 feedback loop has been described in humans (64, 65), suggesting that there may be an analogous pathway in chicken and that the viral protein Meq may trigger the deregulation of this autoregulatory feedback loop.

## ACKNOWLEDGMENTS

We thank Jennifer Labaille and Elodie Boissel (TLVI-EVIL, Université de Tours) for *in vivo* experiment samples. We thank Ali Fendri and Béatrice Chane-Woon-Ming (IBMC-CNRS, Strasbourg, France) for small RNA library construction and bioinformatic analysis. We also thank Yves Le Vern (IASP, INRA, Tours, Nouzilly, France) for assisting us with the flow cytometry analysis.

This work was supported by the Ligue Nationale contre le Cancer, Comité du Cher, Comité de l'Indre; the Fonds Européen de Développement Régional (FEDER) EXMIR (no. 2835-34204); and the Agence Nationale de la Recherche (ANR-07-MIME-012-01).

## REFERENCES

1. **Burgess SC, Young JR, Baaten BJ, Hunt L, Ross LN, Parcells MS, Kumar PM, Tregaskes CA, Lee LF, Davison TF.** 2004. Marek's disease is a natural model for lymphomas overexpressing Hodgkin's disease antigen (CD30). Proc. Natl. Acad. Sci. U. S. A. **101**:13879–13884.
2. **Buckmaster AE, Scott SD, Sanderson MJ, Boursnell ME, Ross NL, Binns MM.** 1988. Gene sequence and mapping data from Marek's disease virus and herpesvirus of turkeys: implications for herpesvirus classification. J. Gen. Virol. **69**(Pt 8):2033–2042.
3. **Lee LF, Wu P, Sui D, Ren D, Kamil J, Kung HJ, Witter RL.** 2000. The complete unique long sequence and the overall genomic organization of the GA strain of Marek's disease virus. Proc. Natl. Acad. Sci. U. S. A. **97**:6091–6096.
4. **Jones D, Lee L, Liu JL, Kung HJ, Tillotson JK.** 1992. Marek disease virus encodes a basic-leucine zipper gene resembling the fos/jun oncogenes that is highly expressed in lymphoblastoid tumors. Proc. Natl. Acad. Sci. U. S. A. **89**:4042–4046.
5. **Qian Z, Brunovskis P, Rauscher F III, Lee L, Kung HJ.** 1995. Transactivation activity of Meq, a Marek's disease herpesvirus bZIP protein persistently expressed in latently infected transformed T cells. J. Virol. **69**: 4037–4044.
6. **Levy AM, Izumiya Y, Brunovskis P, Xia L, Parcells MS, Reddy SM, Lee L, Chen HW, Kung HJ.** 2003. Characterization of the chromosomal binding sites and dimerization partners of the viral oncoprotein Meq in Marek's disease virus-transformed T cells. J. Virol. **77**:12841–12851.
7. **Ajithdoss DK, Reddy SM, Suchodolski PF, Lee LF, Kung HJ, Lupiani B.** 2009. In vitro characterization of the Meq proteins of Marek's disease virus vaccine strain CVI988. Virus Res. **142**:57–67.
8. **Suchodolski PF, Izumiya Y, Lupiani B, Ajithdoss DK, Gilad O, Lee LF, Kung HJ, Reddy SM.** 2009. Homodimerization of Marek's disease virus-encoded Meq protein is not sufficient for transformation of lymphocytes in chickens. J. Virol. **83**:859–869.
9. **Levy AM, Gilad O, Xia L, Izumiya Y, Choi J, Tsalenko A, Yakhini Z, Witter R, Lee L, Cardona CJ, Kung HJ.** 2005. Marek's disease virus Meq transforms chicken cells via the v-Jun transcriptional cascade: a converging transforming pathway for avian oncoviruses. Proc. Natl. Acad. Sci. U. S. A. **102**:14831–14836.
10. **Burnside J, Bernberg E, Anderson A, Lu C, Meyers BC, Green PJ, Jain N, Isaacs G, Morgan RW.** 2006. Marek's disease virus encodes microRNAs that map to Meq and the latency-associated transcript. J. Virol. **80**:8778–8786.
11. **Strassheim S, Stik G, Rasschaert D, Laurent S.** 2012. mdv1-miR-M7-5p, located in the newly identified first intron of the latency-associated transcript of Marek's disease virus, targets the immediate-early genes ICP4 and ICP27. J. Gen. Virol. **93**(Pt 8):1731–1742.
12. **Luo J, Sun AJ, Teng M, Zhou H, Cui ZZ, Qu LH, Zhang GP.** 2011. Expression profiles of microRNAs encoded by the oncogenic Marek's disease virus reveal two distinct expression patterns in vivo during different phases of disease. J. Gen. Virol. **92**:608–620.
13. **Yao Y, Zhao Y, Smith LP, Lawrie CH, Saunders NJ, Watson M, Nair V.** 2009. Differential expression of microRNAs in Marek's disease virus-transformed T-lymphoma cell lines. J. Gen. Virol. **90**:1551–1559.
14. **Muylkens B, Coupeau D, Dambrine G, Trapp S, Rasschaert D.** 2010. Marek's disease virus microRNA designated Mdv1-pre-miR-M4 targets both cellular and viral genes. Arch. Virol. **155**:1823–1837.
15. **Zhao Y, Yao Y, Xu H, Lambeth L, Smith LP, Kgosana L, Wang X, Nair**

**V.** 2009. A functional microRNA-155 ortholog encoded by the oncogenic Marek's disease virus. J. Virol. **83**:489–492.
16. **Zhao Y, Xu H, Yao Y, Smith LP, Kgosana L, Green J, Petherbridge L, Baigent SJ, Nair V.** 2011. Critical role of the virus-encoded microRNA-155 ortholog in the induction of Marek's disease lymphomas. PLoS Pathog. **7**:e1001305. doi:10.1371/journal.ppat.1001305.
17. **Xu S, Xue C, Li J, Bi Y, Cao Y.** 2011. Marek's disease virus type 1 microRNA miR-M3 suppresses cisplatin-induced apoptosis by targeting Smad2 of the transforming growth factor beta signal pathway. J. Virol. **85**:276–285.
18. **Eis PS, Tam W, Sun L, Chadburn A, Li Z, Gomez MF, Lund E, Dahlberg JE.** 2005. Accumulation of miR-155 and BIC RNA in human B cell lymphomas. Proc. Natl. Acad. Sci. U. S. A. **102**:3627–3632.
19. **Metzler M, Wilda M, Busch K, Viehmann S, Borkhardt A.** 2004. High expression of precursor microRNA-155/BIC RNA in children with Burkitt lymphoma. Genes Chromosomes Cancer **39**:167–169.
20. **Gottwein E, Mukherjee N, Sachse C, Frenzel C, Majoros WH, Chi JT, Braich R, Manoharan M, Soutschek J, Ohler U, Cullen BR.** 2007. A viral microRNA functions as an orthologue of cellular miR-155. Nature **450**: 1096–1099.
21. **Morgan R, Anderson A, Bernberg E, Kamboj S, Huang E, Lagasse G, Isaacs G, Parcells M, Meyers BC, Green PJ, Burnside J.** 2008. Sequence conservation and differential expression of Marek's disease virus microRNAs. J. Virol. **82**:12213–12220.
22. **Lambeth LS, Yao Y, Smith LP, Zhao Y, Nair V.** 2009. MicroRNAs 221 and 222 target p27Kip1 in Marek's disease virus-transformed tumour cell line MSB-1. J. Gen. Virol. **90**:1164–1171.
23. **Kumarswamy R, Volkmann I, Thum T.** 2011. Regulation and function of miRNA-21 in health and disease. RNA Biol. **8**:706–713.
24. **Fujita S, Ito T, Mizutani T, Minoguchi S, Yamamichi N, Sakurai K, Iba H.** 2008. miR-21 gene expression triggered by AP-1 is sustained through a double-negative feedback mechanism. J. Mol. Biol. **378**:492–504.
25. **Loffler D, Brocke-Heidrich K, Pfeifer G, Stocsits C, Hackermüller J, Kretzschmar AK, Burger R, Gramatzki M, Blumert C, Bauer K, Cvijic H, Ullmann AK, Stadler PF, Horn F.** 2007. Interleukin-6 dependent survival of multiple myeloma cells involves the Stat3-mediated induction of microRNA-21 through a highly conserved enhancer. Blood **110**:1330–1333.
26. **Wang K, Li PF.** 2010. FoxO3a regulates apoptosis by negatively targeting miR-21. J. Biol. Chem. **285**:16958–16966.
27. **Asangani IA, Rasheed SA, Nikolova DA, Leupold JH, Colburn NH, Post S, Allgayer H.** 2008. MicroRNA-21 (miR-21) post-transcriptionally downregulates tumor suppressor Pdcd4 and stimulates invasion, intravasation and metastasis in colorectal cancer. Oncogene **27**:2128–2136.
28. **Meng F, Henson R, Wehbe-Janek H, Ghoshal K, Jacob ST, Patel T.** 2007. MicroRNA-21 regulates expression of the PTEN tumor suppressor gene in human hepatocellular cancer. Gastroenterology **133**:647–658.
29. **Akiyama Y, Kato S, Iwa N.** 1973. Continuous cell culture from lymphoma of Marek's disease. Biken J. **16**:177–179.
30. **Hirai K, Yamada M, Arao Y, Kato S, Nii S.** 1990. Replicating Marek's disease virus (MDV) serotype 2 DNA with inserted MDV serotype 1 DNA sequences in a Marek's disease lymphoblastoid cell line MSB1-41C. Arch. Virol. **114**:153–165.
31. **Baba TW, Giroir BP, Humphries EH.** 1985. Cell lines derived from avian lymphomas exhibit two distinct phenotypes. Virology **144**:139–151.
32. **Mazzella O, Cauchy L, Coudert F, Richard J.** 1986. Chicken thymocyte-specific antigens identified by monoclonal antibodies: characterization and distribution in normal tissues and in tumoral tissues from Marek's disease chicken. Hybridoma **5**:319–328.
33. **Djeraba-AitLounis A, Soubieux D, Klapper W, Rasschaert D.** 2004. Induction of telomerase activity in avian lymphoblastoid cell line transformed by Marek's disease virus, MDCC-MSB1. Vet. Pathol. **41**:405–407.
34. **Pfeffer S, Sewer A, Lagos-Quintana M, Sheridan R, Sander C, Grässer FA, van Dyk LF, Ho CK, Shuman S, Chien M, Russo JJ, Ju J, Randall G, Lindenbach BD, Rice CM, Simon V, Ho DD, Zavolan M, Tuschl T.** 2005. Identification of microRNAs of the herpesvirus family. Nat. Methods **2**:269–276.
35. **Stik G, Laurent S, Coupeau D, Coutaud B, Dambrine G, Rasschaert D, Muylkens B.** 2010. A p53-dependent promoter associated with polymorphic tandem repeats controls the expression of a viral transcript encoding clustered microRNAs. RNA **16**:2263–2276.
36. **Raymond CK, Roberts BS, Garrett-Engele P, Lim LP, Johnson JM.** 2005. Simple, quantitative primer-extension PCR assay for direct monitoring of microRNAs and short-interfering RNAs. RNA **11**:1737–1744.
37. **Yao Y, Zhao Y, Xu H, Smith LP, Lawrie CH, Watson M, Nair V.** 2008. MicroRNA profile of Marek's disease virus-transformed T-cell line MSB-1: predominance of virus-encoded microRNAs. J. Virol. **82**:4007–4015.
38. **Debba-Pavard M, Ait-Lounis A, Soubieux D, Rasschaert D, Dambrine G.** 2008. Vaccination against Marek's disease reduces telomerase activity and viral gene transcription in peripheral blood leukocytes from challenged chickens. Vaccine **26**:4904–4912.
39. **Chang KS, Ohashi K, Onuma M.** 2002. Diversity (polymorphism) of the meq gene in the attenuated Marek's disease virus (MDV) serotype 1 and MDV-transformed cell lines. J. Vet. Med. Sci. **64**:1097–1101.
40. **Spatz SJ, Petherbridge L, Zhao Y, Nair V.** 2007. Comparative full-length sequence analysis of oncogenic and vaccine (Rispens) strains of Marek's disease virus. J. Gen. Virol. **88**:1080–1096.
41. **Chang KS, Ohashi K, Onuma M.** 2002. Suppression of transcription activity of the MEQ protein of oncogenic Marek's disease virus serotype 1 (MDV1) by L-MEQ of non-oncogenic MDV1. J. Vet. Med. Sci. **64**:1091–1095.
42. **Smale ST, Kadonaga JT.** 2003. The RNA polymerase II core promoter. Annu. Rev. Biochem. **72**:449–479.
43. **Frith MC, Valen E, Krogh A, Hayashizaki Y, Carninci P, Sandelin A.** 2008. A code for transcription initiation in mammalian genomes. Genome Res. **18**:1–12.
44. **Iliopoulos D, Jaeger SA, Hirsch HA, Bulyk ML, Struhl K.** 2010. STAT3 activation of miR-21 and miR-181b-1 via PTEN and CYLD are part of the epigenetic switch linking inflammation to cancer. Mol. Cell **39**:493–506.
45. **Mudduluru G, George-William JN, Muppala S, Asangani IA, Kumarswamy R, Nelson LD, Allgayer H.** 2011. Curcumin regulates miR-21 expression and inhibits invasion and metastasis in colorectal cancer. Biosci. Rep. **31**:185–197.
46. **Chinenov Y, Kerppola TK.** 2001. Close encounters of many kinds: Fos-Jun interactions that mediate transcription regulatory specificity. Oncogene **20**:2438–2452.
47. **McBride K, Nemer M.** 1998. The C-terminal domain of c-fos is required for activation of an AP-1 site specific for jun-fos heterodimers. Mol. Cell. Biol. **18**:5073–5081.
48. **Janknecht R, Nordheim A.** 1993. Gene regulation by Ets proteins. Biochim. Biophys. Acta **1155**:346–356.
49. **Klemsz MJ, McKercher SR, Celada A, Van Beveren C, Maki RA.** 1990. The macrophage and B cell-specific transcription factor PU.1 is related to the ets oncogene. Cell **61**:113–124.
50. **Brown AC, Smith LP, Kgosana L, Baigent SJ, Nair V, Allday MJ.** 2009. Homodimerization of the Meq viral oncoprotein is necessary for induction of T-cell lymphoma by Marek's disease virus. J. Virol. **83**:11142–11151.
51. **Lupiani B, Lee LF, Cui X, Gimeno I, Anderson A, Morgan RW, Silva RF, Witter RL, Kung HJ, Reddy SM.** 2004. Marek's disease virus-encoded Meq gene is involved in transformation of lymphocytes but is dispensable for replication. Proc. Natl. Acad. Sci. U. S. A. **101**:11815–11820.
52. **Qian Z, Brunovskis P, Lee L, Vogt PK, Kung HJ.** 1996. Novel DNA binding specificities of a putative herpesvirus bZIP oncoprotein. J. Virol. **70**:7161–7170.
53. **Brown AC, Baigent SJ, Smith LP, Chattoo JP, Petherbridge LJ, Hawes P, Allday MJ, Nair V.** 2006. Interaction of MEQ protein and C-terminal-binding protein is critical for induction of lymphomas by Marek's disease virus. Proc. Natl. Acad. Sci. U. S. A. **103**:1687–1692.
54. **Fei J, Li Y, Zhu X, Luo X.** 2012. miR-181a post-transcriptionally downregulates oncogenic RalA and contributes to growth inhibition and apoptosis in chronic myelogenous leukemia (CML). PLoS One **7**:e32834. doi:10.1371/journal.pone.0032834.
55. **Huang L, Lin JX, Yu YH, Zhang MY, Wang HY, Zheng M.** 2012. Downregulation of six microRNAs is associated with advanced stage, lymph node metastasis and poor prognosis in small cell carcinoma of the cervix. PLoS One **7**:e33762. doi:10.1371/journal.pone.0033762.
56. **Nadiminty N, Tummala R, Lou W, Zhu Y, Shi XB, Zou JX, Chen H, Zhang J, Chen X, Luo J, deVere White RW, Kung HJ, Evans CP, Gao AC.** 2012. MicroRNA let-7c is downregulated in prostate cancer and suppresses prostate cancer growth. PLoS One **7**:e32832. doi:10.1371/journal.pone.0032832.
57. **Xu XM, Wang XB, Chen MM, Liu T, Li YX, Jia WH, Liu M, Li X, Tang**

**H.** 2012. MicroRNA-19a and -19b regulate cervical carcinoma cell proliferation and invasion by targeting CUL5. Cancer Lett. **322**:148–158.
58. **Baigent SJ, Smith LP, Petherbridge LJ, Nair VK.** 2011. Differential quantification of cloned CVI988 vaccine strain and virulent RB-1B strain of Marek's disease viruses in chicken tissues, using real-time PCR. Res. Vet. Sci. **91**:167–174.
59. **Mrazek J, Kreutmayer SB, Grasser FA, Polacek N, Huttenhofer A.** 2007. Subtractive hybridization identifies novel differentially expressed ncRNA species in EBV-infected human B cells. Nucleic Acids Res. **35**:e73. doi: 10.1093/nar/gkm244.
60. **Tsai YH, Wu MF, Wu YH, Chang SJ, Lin SF, Sharp TV, Wang HW.** 2009. The M type K15 protein of Kaposi's sarcoma-associated herpesvirus regulates microRNA expression via its SH2-binding motif to induce cell migration and invasion. J. Virol. **83**:622–632.
61. **Frankel LB, Christoffersen NR, Jacobsen A, Lindow M, Krogh A, Lund AH.** 2008. Programmed cell death 4 (PDCD4) is an important functional target of the microRNA miR-21 in breast cancer cells. J. Biol. Chem. **283**: 1026–1033.
62. **Yao T, Lin Z.** 2012. MiR-21 is involved in cervical squamous cell tumorigenesis and regulates CCL20. Biochim. Biophys. Acta **1822**:248–260.
63. **Yamakuchi M, Ferlito M, Lowenstein CJ.** 2008. miR-34a repression of SIRT1 regulates apoptosis. Proc. Natl. Acad. Sci. U. S. A. **105**:13421–13426.
64. **Talotta F, Cimmino A, Matarazzo MR, Casalino L, De Vita G, D'Esposito M, Di Lauro R, Verde P.** 2009. An autoregulatory loop mediated by miR-21 and PDCD4 controls the AP-1 activity in RAS transformation. Oncogene **28**:73–84.
65. **Zhu Q, Wang Z, Hu Y, Li J, Li X, Zhou L, Huang Y.** 2012. miR-21 promotes migration and invasion by the miR-21-PDCD4-AP-1 feedback loop in human hepatocellular carcinoma. Oncol. Rep. **27**:1660–1668.